JOURNAL OF MATERIALS SCIENCE 25 (1990) 3649–3658

Precipitation of ultrafine powders of zirconia polymorphs and their conversion to $MZrO_3$ (M = Ba, Sr, Ca) by the hydrothermal method

T. R. N. KUTTY, R. VIVEKANANDAN, SAM PHILIP
Materials Research Centre, Indian Institute of Science, Bangalore 560 012, India

Ultrafine powders of ZrO_2 with a high degree of crystallinity and chemical purity are hydrothermally precipitated from aqueous solutions of impure zirconyl oxychloride or the acid extract of zircon ($ZrSiO_4$)-frit at 2 to 8 MPa and 180 to 230° C. Monoclinic ZrO_2 is produced from aqueous hydrochloric acid, whereas tetragonal ZrO_2 is formed from the same medium when sulphate ions are present with $[SO_4^{2-}]/[Cl^-] \geqslant 0.08$. If cation impurities such as Y^{3+} or Ce^{3+} are incorporated, the stability range of the tetragonal phase is extended to higher temperatures. Ultrafine powders are characterized by X-ray broadening methods, TEM and thermally as well as mechanically induced transformation characteristics. The tetragonal ZrO_2 powder is constituted of polydomain crystallites with higher hydroxyl ion content than the monoclinic phase. Both series of powders convert to $BaZrO_3$, $SrZrO_3$ or $CaZrO_3$ perovskites when suspended in the corresponding hydroxide solution at 190 to 480° C and 2 to 100 MPa.

1. Introduction

Ultrafine powders of simple or complex oxides with high purity, narrow particle size distribution, phase homogeneity, controlled particle morphology and a high degree of crystallinity can be produced by the hydrothermal process. The method involves heating the aqueous suspensions in a closed vessel above the boiling point of water at pressures greater than 0.1 MPa. Because the hydrothermal processes are chemical reactions involving no additional precipitants except H_2O, the oxides are formed as single-crystal particles. The starting materials are inexpensive and easy to handle metal salts or the acid extraction of the corresponding source minerals. The other advantages of hydrothermal crystallization are the reduced energy costs by way of the moderate temperatures used for the process, lower pollution and simplicity of the processing equipment. The disadvantages are the necessity to use pressurized equipment and corrosion problems. However, more recent developments in technology have helped to overcome these problems so that hydrothermal process is emerging as an important non-conventional technique for the production of fine oxide powders. The fact that nearly quantitative precipitation can be achieved from the impure acidic feedstock solutions at shorter durations to yield high-purity oxides, requiring no post-preparative grinding, renders the hydrothermal technique very attractive for up-grading to the industrial scale.

Through a series of investigations we have shown that ultrafine powders of perovskites such as $MTiO_3$, $MZrO_3$ and $MSnO_3$ (M = barium, calcium, strontium or lead) with high-phase singularity can be obtained directly by the hydrothermal method [1–7]. In these cases the starting materials are hydrated gels of TiO_2, ZrO_2 or SnO_2 and the corresponding $M(OH)_2$. In our continued efforts to reduce the number of steps involved in these preparations so that a viable commercial process can be developed, the hydrated gel of titania has been replaced by ultrafine powders of TiO_2 [8]. Starting from commercially available $TiCl_4$, we have observed that fine powders of high-purity rutile as well as anatase forms of TiO_2 can be hydrothermally produced [8]. At present, we have extended these investigations for the preparation of ultrafine powders of ZrO_2 using impure $ZrOCl_2$ or the acid (HCl) extract of zircon-frit formed from the reactions of sodium hydroxide and zircon sand. We have observed that predominantly the monoclinic form of ZrO_2 is produced from aqueous HCl medium, whereas tetragonal ZrO_2 is formed in the same solution when sulphate ion impurities are present. If cation impurities such as Y^{3+} or Ce^{3+} are incorporated, the stability range of the tetragonal phase is extended to higher temperatures. Further, these fine powders of ZrO_2 could be converted to $MZrO_3$ through the reaction with $M(OH)_2$ under hydrothermal conditions.

Currently there is considerable interest in toughened zirconia [9, 10]. Together with toughness and strength, zirconia possess good wear resistance, hardness and thermal shock resistance so that zirconia-containing components find wider engineering applications. The key to the properties of these components lies in the controlled transformation of the metastable phases to the stabler monoclinic phases. In addition to the partially or fully stabilized cubic ZrO_2, the tetragonal phase is more important because of its martensitic transition to monoclinic ZrO_2. Although there are

0022–2461/90 $03.00 + .12

many reports on the low-temperature crystallization of various polymorphs [11–14], preparation of phase-pure tetragonal ZrO_2 is more difficult to reproduce than stated. Hydrothermal treatment of zirconia gel in neutral or alkaline media leads to tetragonal plus monoclinic phases [15]. Nishizawa *et al.* [16] studied the effect of mineralizers on the crystallization of ZrO_2 under hydrothermal conditions. However, these attempts are limited by the fact that the original impurities are retained in the product and therefore cannot yield high-purity ZrO_2, unlike that from acid solutions. Although Cypres and Raucq [11] proposed that anion impurities may stabilize the tetragonal ZrO_2 at room temperature, there seems to be no general agreement on the mechanism of metastability. In addition to the influence of impurities [11–14], a particle size effect as well as the role of surface energy are reported as alternative factors for the stability of the tetragonal phase [17–20].

2. Experimental procedure

2.1. Conditions of hydrothermal precipitation

Aqueous zirconium oxychloride (0.5 to 2 M in 3 M HCl) was charged (65% to 70% fill) into a teflon (PTFE)-lined, Morey-type hydrothermal vessel (SS 304) of 150 ml capacity fitted with a stirrer and pressure gauge through an isolation diaphragm, in order to avoid direct contact of the Bourdon-tube with the corrosive fluids. The autoclave was maintained at the desired temperature between 180 and 250° C for 0.25 to 2 h. The pressure remained close to the values reported for the HCl–H_2O system (2.0 to 10 MPa) [21]. ZrO_2 fine powders, thus obtained, were washed free of chloride ions by decantation. With multiple washings the products tend to become colloidal suspensions, as the pH is increased above 5.5. This could be avoided if the aqueous zirconium oxychloride contained low concentrations of sulphuric acid. The resulting ZrO_2 fine powders settle down faster and could be washed free of anions completely and were oven dried at 110° C.

Impure zirconium oxychloride solutions were obtained from zirconia-frit by leaching with HCl. Zircon-frit was obtained by fusing fine zircon ($ZrSiO_4$) sand (300 mesh) with NaOH at 1000° C in nickel containers. The resulting solutions were filtered to remove insoluble materials and boiled until traces of fine silica separated out. The clear solution was hydrothermally treated at 180° C whereupon ZrO_2 precipitation took place. Here again, the presence of sulphuric acid in low concentration was effective in faster settling and easy washing to the precipitate.

Ultrafine powders of ZrO_2 from either of the above methods were suspended in $Ba(OH)_2$ or $Sr(OH)_2$ solution or in an aqueous slurry of reactive (carbonate-free) CaO so that the Zr/M ratio remains close to 0.97 to 1.03. These mixtures were heated in the hydrothermal vessel. Because the reaction between ultrafine powders of ZrO_2 and $Sr(OH)_2$ or $Ca(OH)_2$ was slow and incomplete in the above temperature range, the mixtures were heated at 280 to 480° C. In such cases, the reactants were directly filled in the autoclave without the liner and the products were not contaminated because corrosion by the alkaline media was slow and ineffective. In all these experiments the pressure remained close to the saturated vapour pressure of water below 300° C and reached 100 MPa at 480° C, depending upon the percentage fill. The resulting products were washed with CO_2-free distilled water to remove any excess $M(OH)_2$. The free-flowing $MZrO_3$ powders were oven-dried. They were analysed by wet chemical methods.

2.2. Methods of characterization

Phase identification was carried out by X-ray powder diffraction using a Philips 1050/70 diffractometer. The volume fraction (v_m) of monoclinic zirconia in a mixed-phase sample was estimated using the formula [22]

$$v_m = \frac{PX_m}{1 + (P + 1)X_m} \quad (1)$$

where

$$X_m = \frac{I_m(1\,1\,1) + I_m(1\,1\,\bar{1})}{I_m(1\,1\,1) + I_m(1\,1\,\bar{1}) + I_t(1\,1\,1)} \quad (2)$$

I_m and I_t are the integrated intensities of monoclinic and tetragonal phases, respectively. P is a numerical constant (1.311), as given in [22]. For measuring the X-ray line-broadening, a Rigaku Denki powder diffractomer was used which was equipped with quartz monochromator and rotating anode operating at 50 kV and 190 mA. The data were gathered using strictly monochromatic Cu$K\alpha_1$ radiation (λ = 0.154 06 nm) by a step-scan mode with $2\theta = 0.01°$ per step. The data were plotted on a X-ray diagram with extended scale so that $2\theta = 1°$ corresponds to 10 cm, from which the accuracy of measured peak-width could be at least ± 0.01 in 2θ. The data were corrected for polarization and Lorentz factor and the background obtained by the procedure of least squares was subtracted. A highly crystalline sample of ZrO_2 (monoclinic) heated at 1100° C for 48 h was used to determine the instrumental line-broadening. The breadth of the diffraction peak at half maximum ($\beta_{1/2}$) was dependent on crystallite size and microstrains in the lattice. The values of the apparent size and the lattice strains in the direction perpendicular to specific crystallographic planes were obtained by the Williamson–Hall method, assuming that the size- and strain-factors gave rise to Cauchy peak-profile [23]. Alternatively, a Gaussian peak profile was also attempted [24]. The size- and strain-broadening of the X-ray diffraction lines were also analysed by the Warren–Averbach [25] method, modified by Delhez and Mittemeijer [26]. Deconvolution of the experimental profiles in the Fourier analysis was carried out by Stokes method [27].

Particle size and morphology were also studied by transmission electron microscopy (TEM) using a Philips EM 301. The powders were ultrasonically dispersed in acetone and were mounted on a carbon film supported on a copper grid. A large number of micrographs was obtained for each sample. The mean particle size distribution was measured on enlargements by the intercept method. The microscope magnification was calibrated using the replica of a cross-grating with

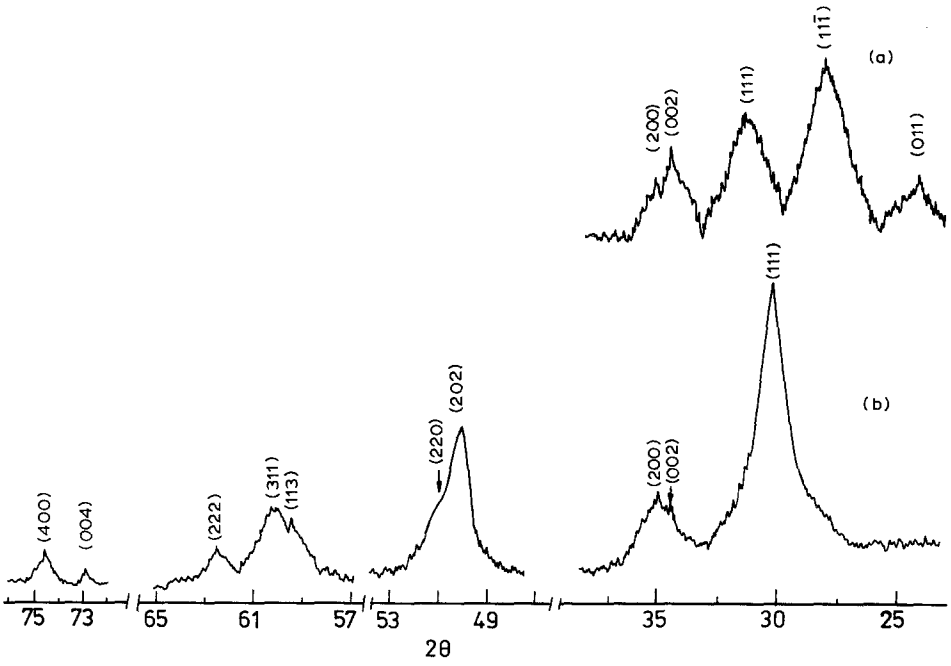

Figure 1 Part of the X-ray diffraction patterns of (a) monoclinic ZrO_2, (b) tetragonal ZrO_2 prepared at 200° C with $[SO_4^{2-}/Cl^-] = 0.08$.

2160 lines/mm. Simultaneous TGA/DTA was carried out with a Sinku Riko TA 1500 thermal analyser. The infrared (IR) spectra were recorded with a Perkin–Elmer 597 spectrometer. The amount of impurity in the powder was determined by atomic absorption spectrophotometry (AAS), using a Perkin–Elmer 2380 instrument.

3. Results

3.1. Phase content of ZrO_2 powders

Fine powders of ZrO_2 begin to form within 15 min from zirconium oxychloride in 1 to 3 M HCl at 180° C. The precipitation is quantitative after ~1 h, because no Zr^{4+} is detected in the residual solution. X-ray diffractograms of fine ZrO_2 powders show complete monoclinic character (Fig. 1a). The extensive line broadening for all the reflections is indicative of the low particle size of these powders. The quantitative analysis of the line broadening is presented in the next section. TGA of ZrO_2 formed at 180° C shows ~0.4% weight loss in the range 180 to 300° C and the weight remained unchanged at higher temperatures. The corresponding endotherm in DTA is very shallow. No exothermic peak arising from the crystallization of any amorphous faction is observed up to 1200° C in DTA. Chemical analysis of the evolved gases during thermal treatment in air of ZrO_2 powders, hydrothermally prepared at 180° C, shows only H_2O. The infrared spectrum of this sample has a broad absorption in the ~3650 to 3300 cm^{-1} region and no absorption band at ~1650 cm^{-1} is observed. This result indicates that mostly hydroxyl ions are present as the residual impurity.

ZrO_2 prepared above 200° C has < 0.05% weight loss. There are only marginal changes in the unit cell parameters of the product with increasing crystallization temperature. ZrO_2 (monoclinic) from the hydrothermal precipitation at 180° C has $a_0 = 0.5150$, $b_0 = 0.5213$ and $c_0 = 0.5325$ nm and $\beta = 99°$, whereas the product prepared at 220° C has $a_0 = 0.5146$, $b_0 = 0.5203$ and $c_0 = 0.5316$ nm and $\beta = 99°10'$. The presence of dilute H_2SO_4 in the aqueous zirconium oxychloride not only eliminates the tendency to form colloid during washing of the hydrothermal product, but also changes the phase content. The X-ray diffractogram of ZrO_2 shows that it is fully tetragonal (Fig. 1b).

Formation of the tetragonal phase is also observed with the addition of $(NH_4)_2SO_4$ in the place of H_2SO_4 so that it is positively due to the presence of SO_4^{2-} ions in the hydrothermal medium. Further, formation of mixed monoclinic and tetragonal phases is noticed with decreasing relative concentration of $[SO_4^{2-}/Cl^-]$. The concentration of chloride ions is calculated by assuming that 1 mol $ZrOCl_2$ gives rise to 2 mol Cl^- which is over and above the concentration of HCl added. When SO_4^{2-}/Cl^- is greater than 0.08 in the starting solution, the tetragonal phase is fully stabilized (Fig. 2). However, if this ratio is greater than 0.25, no precipitation of ZrO_2 is observed even when the reaction temperature is raised to 280° C. This is also the case when zirconium sulphate is used in place of zirconyl chloride. The influence of the SO_4^{2-} ion is in

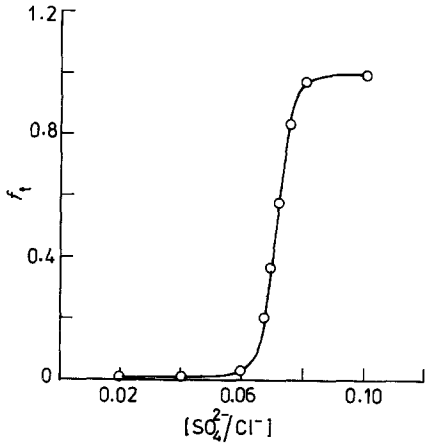

Figure 2 Effect of sulphate ion concentration on the stabilization of tetragonal ZrO_2 phase.

the stage of ZrO_2 precipitation, which is evident from the fact that fine powders of ZrO_2 (monoclinic) remained unchanged when suspended in 0.5 M H_2SO_4 and heated at 200° C in the pressure vessel. Conversely, tetragonal ZrO_2 formed hydrothermally, remains stable in the presence of 0.5 M HCl under the same experimental conditions.

Fig. 1b illustrates the X-ray diffraction traces of the tetragonal powder. Owing to line broadening, closely spaced pairs of reflections such as (0 0 2) and (2 0 0), (2 0 2) and (2 2 0), (1 1 3) and (3 1 1) are partially overlapping. However, their features are clear enough to distinguish the tetragonal from the cubic phase. Using the higher angle reflections, the cell parameter of the tetragonal phase has been calculated which yields $a_0 = 0.5128$ and $c_0 = 0.5159$ nm. The d-spacing observed for the (1 1 1) reflection is 0.2963 nm, which can be further compared with $d = 0.2947$ to 0.2952 nm obtained by Mitsuhashi *et al.* [15] and $d = 0.2960$ nm reported by Gupta *et al.* [28]. The slight difference in d-spacing may arise from the presence of hydroxyl ions as indicated by the ~1.5% weight loss in two steps in TGA, namely ~200 to 300° C (~0.3% weight loss) and 560 to 650° C (~1.2% weight loss). The broad infrared absorption ~3650 to 3300 cm^{-1} arising from the OH stretching vibrations is stronger for the tetragonal phase than for monoclinic ZrO_2.

3.2. X-ray line broadening

The slope and intercept of the Williamson–Hall plots are related to the root mean square of the lattice strains and the mean size of the crystallites, respectively. The results obtained from the Williamson–Hall plots of the pairs of reflections (1 1 1), (2 2 2) and (2 0 0), (4 0 0) showed that the mean size of the crystallite is smaller in the [1 0 0], than those in the [1 1 1] (Table I). The Williamson–Hall plot also showed that the values of lattice strains from (2 0 0), (4 0 0) reflections are smaller than the values deduced for the (1 1 1), (2 2 2) pair. This is true for both tetragonal and monoclinic ZrO_2 obtained by the hydrothermal method, as is evident from the values given in Table I. For the Warren–Averbach analysis, the Fourier cosine coefficient $A(n)$, is expressed as a function of distance L in the direction perpendicular to the diffracting planes so that

$$L = \frac{n\lambda}{2(\sin\theta_2 - \sin\theta_1)} \quad (3)$$

where λ is the wavelength, n the Fourier harmonic number, θ_1 and θ_2 are the limits over which the reflections are recorded, allowance being made for the "hook effect" for small values of L. The separation of size and strain broadening by the Warren–Averbach method is based on the relation [26]

$$A(n, L) = A(n) - A(n)2\pi^2L^2\langle e^2(n)\rangle \quad (4)$$

where $A(n)$ is the size Fourier coefficient and $\langle e^2(n)\rangle$ is the strain. $A(n)$ and $\langle e_2(n)\rangle$ are evaluated from the plot of $A(n)$ against L^2 for two orders of reflections (Table I). The initial slope of the Fourier cosine coefficient curves (Fig. 3) gives the values for the mean apparent size in the perpendicular direction.

From the data in Table I it is evident that the crystallite sizes of the tetragonal phase are larger than those of the monoclinic ZrO_2, even though they are prepared under identical conditions except for the presence of SO_4^{2-} ions in the former case. Hannink *et al.* [29] have shown that there is a critical crystallite size for the tetragonal phase that can remain stable at a given temperature. If the particle size of the tetragonal ZrO_2 is above this value, spontaneous transformation to monoclinic phase takes place. It is possible that under hydrothermal conditions the size factor does not contribute to the stability of the tetragonal phase.

3.3. ZrO_2 powders from zircon

The superiority of the hydrothermal crystallization over the conventional methods is in the easily attainable purity of the resulting ZrO_2 powders. This is due to the fact that the precipitation takes place from the strongly acidic solutions. Therefore, the major fraction of the impurities remains in solution because the segregation coefficient $\gg 1$ for the fluid phases as compared to the crystallizing solid. This is clear from the impurity contents in ZrO_2 powder prepared from zircon-frit by the neutralization procedure. In the latter case, zircon-frit is leached with HCl and the resulting solution is treated with NH_4OH. The precipitate is washed free of chloride and alkali ions and subsequently calcined at 1000° C. The impurity contents of this product are compared in Table II with ZrO_2 fine powders prepared hydrothermally from the same starting solution at 200° C. All the impurities except silicon and titanium have been reduced to p.p.m. levels in the hydrothermal product. Particularly noteworthy is the reduction in concentration of the transition metals. The phase contents of ZrO_2 from zircon-frit follows the same trend as those prepared

TABLE I Size and strain parameters from the X-ray line broadening along [1 1 1] and [1 0 0] directions of ZrO_2 prepared at 200° C

Sample	Cauchy's size, D_c (nm)	Cauchy's strain, e_c ($\times 10^{-3}$)	Gaussian size, D_g (nm)	Gaussian strain, e_g ($\times 10^{-3}$)	Warren–Averbach size (nm)	Warren–Averbach strain, e_{wa} ($\times 10^{-3}$)
ZrO_2 (tet)						
[1 1 1]	9.3	2.5	9.5	1.79	10.0	1.9
[1 0 0]	7.2	2.6	7.8	2.01	9.1	1.6
ZrO_2 (mono)						
[1 1 1]	6.5	2.1	7.2	1.94	8.5	2.2
[1 0 0]	6.2	1.8	6.6	1.75	7.4	1.9

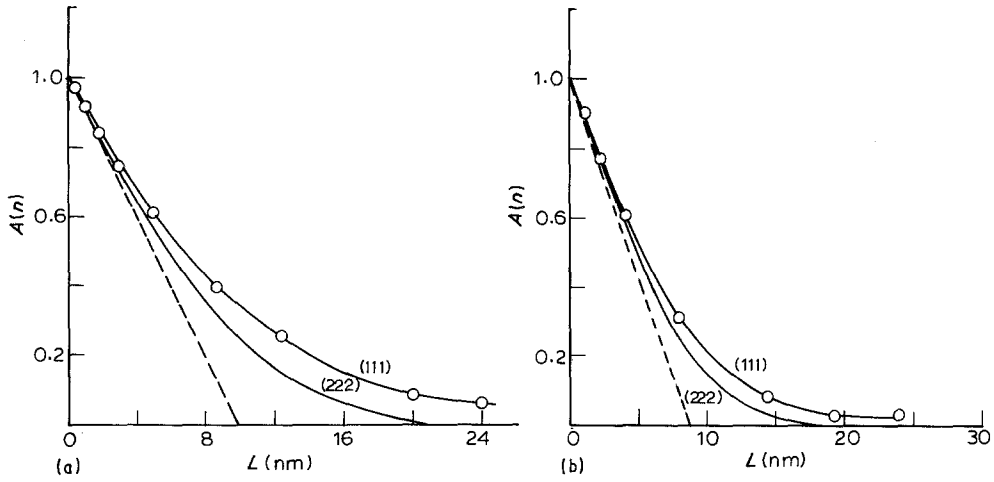

Figure 3 Fourier cosine coefficients, $A(n)$, plotted against L for (a) tetragonal, and (b) monoclinic ZrO_2.

from zirconium oxychloride, specifically with respect to the influence of SO_4^{2-} ions.

3.4. Transmission electron microscopy

TEM studies reveal that hydrothermally prepared ZrO_2 (monoclinic) fine powders contain well-developed prismatic to acicular crystallites terminating in pyramidal phases (Fig. 4a). These crystallites tend to form loose aggregates. Growth habits such as contact twinning or multiple penetration twinning are also observed in these aggregates. Selected-area electron diffraction patterns of individual crystallites show that they are single crystals with monodomain characteristics. The ED patterns with the clinonet symmetry correspond to those of the monoclinic phases (Fig. 4b). The particle size of monoclinic ZrO_2 ranges from 3 to 20 nm in length, having aspect ratios of 2 to 8. The ZrO_2 tetragonal particles prepared in the presence of SO_4^{2-} ions are nearly spherical to irregular-shaped platelets (Fig. 4c). The ED pattern of these particles shows that they are multidomain crystallites (Fig. 4d). The diffraction spots are undistorted with minimum streaking, which indicates that the concentration of line or plane defects is very low. The particle size of the ZrO_2 powder ranges from 8 to 25 nm. Fig. 5 shows the size distribution curves derived from TEM studies for both monoclinic and tetragonal powders. The particle size of the monoclinic phase having acicular morphology, for crystallites, is of larger uncertainty as indicated by the length of the bars in Fig. 5. The X-ray crystallite sizes need not be the same as those from the TEM method because X-ray line broadening is, in addition to the size effect, also caused by strains and by domains within the crystallites that are not taken into account by microscopy. Thus the maxima in the distribution curves (Fig. 5) are somewhat larger than the size values given in Table I. It is also clear from Fig. 5 that the distribution curve for tetragonal ZrO_2 is maximized at a higher size value with a narrower distribution than the monoclinic ZrO_2.

TABLE II Impurity contents (p.p.m.) in ZrO_2 fine powders prepared by neutralization and hydrothermal precipitation

Impurity	Neutralization	Hydrothermal
Ti	30	30
Si	80	90
Fe	6800	40
Ni	60	5
Mn	25	2
Mg	400	3
Al	2300	10
Ca	35	1
Σ REE	80	2

REE = rare earths.

3.5. Thermal treatment and phase transformation characteristics

The tetragonal ZrO_2 metastably retained at temperatures far below the equilibrium transformation temperature undergoes both thermally and mechanically induced transformation to monoclinic ZrO_2 which is the stable phase at lower temperatures. On annealing in air, the hydrothermally prepared tetragonal ZrO_2 undergoes phase transition at $\sim 600°$ C to the monoclinic phase. This is accompanied by the weight loss $\sim 1.2\%$. Evolved gas analysis showed that only H_2O is generated during the transformation. As shown in (Fig. 6a), the tetragonal phase decreases with increase in temperature to $\sim 600°$ C and increasing duration of annealing. The curves in Fig. 6a have different slopes in the early and the late stages of transformation compared to the main part of the phase transformation. Extrapolation of the early regions of the curves to the temperature axis shows that the transformation may incipiently begin at 420° C. The fact that the late-stage regions of the curve run parallel to the temperature axis may point to incomplete transformation even after a long annealing time. The activation energy corresponding to 50% conversion was evaluated to be ~ 543.4 kJ mol^{-1} from the Arrhenius plot of log rate against the reciprocal of the absolute temperature.

In order to study the effect of cations on the metastability of hydrothermally prepared tetragonal ZrO_2, Y^{3+} and Ce^{3+} were used as impurities. However, these cation impurities could not be incorporated in strong acid solutions for the reasons presented in Section 3.3. Therefore, the tetragonal ZrO_2 powder obtained hydrothermally in the presence of SO_4^{2-} ions is suspended in dilute $Y_2(SO_4)_3$ or $Ce_2(SO_4)_3$ solutions and further heated in the pressure vessel at 200° C. Most of Y^{3+} or Ce^{3+} originally present in the medium is found in the

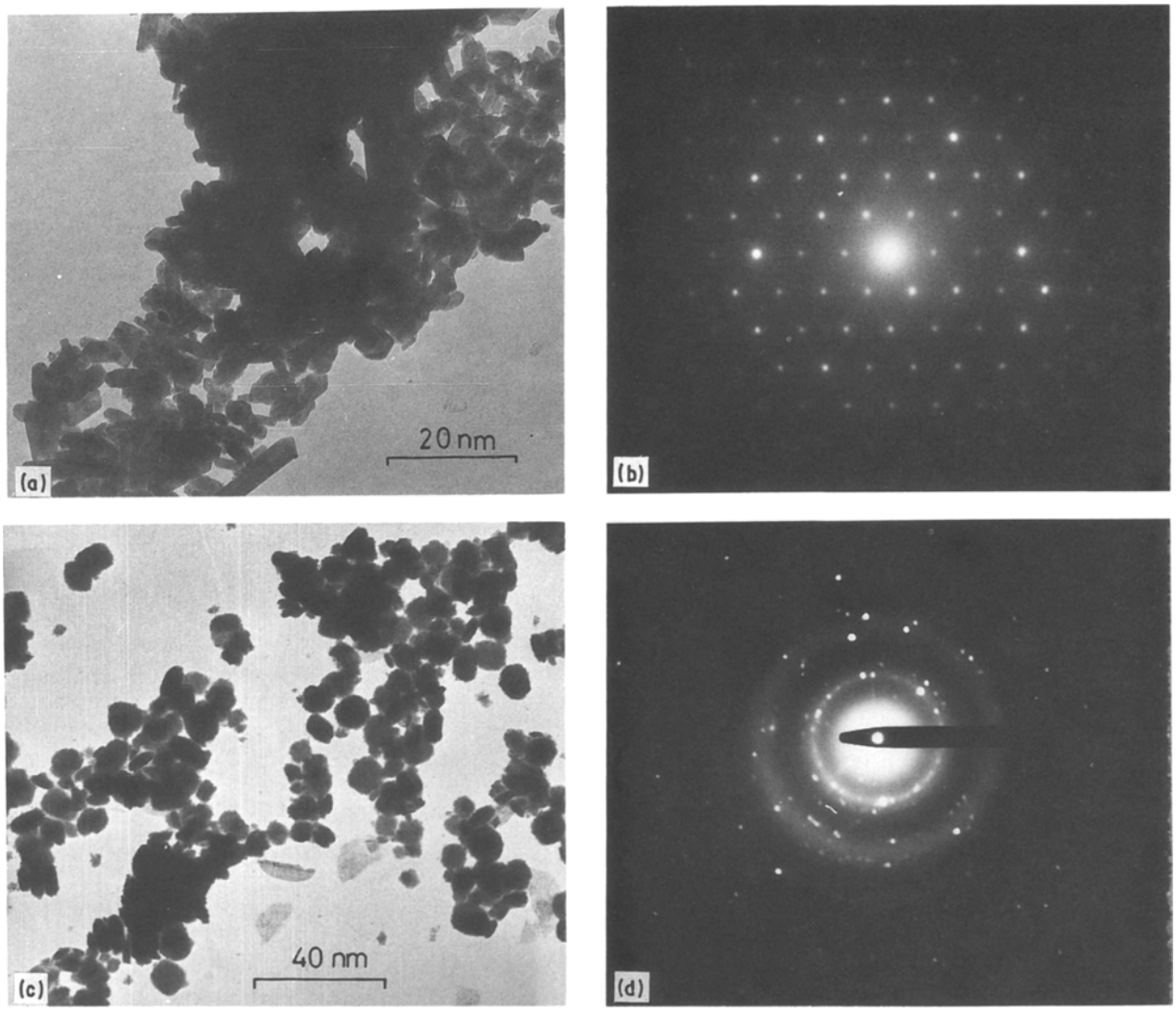

Figure 4 TEM of (a) monoclinic ZrO_2, (b) selected-area electron diffraction pattern of (a), (c) tetragonal ZrO_2 produced with $[SO_4^{2-}/Cl^-] = 0.08$, and (d) selected-area electron diffraction pattern of (c).

powder within the cation concentration of ~1 to 8 wt% of the corresponding oxides, Ln_2O_3 (Ln = lanthanide). The transformation temperature of these powders was raised to the region 1150 to 1450° C (Fig. 6b). In contrast to the transformation behaviour in the absence of cation impurities, the decrease in tetragonal-phase content is continuous and nearly linear with temperature for a given period of annealing. Another difference is the enhanced activation energy of ~668.8 kJ mol^{-1} at 50% conversions, as estimated from the Arrhenius plot. These differences are not due to the changes in crystallite size because the cation-mounted tetragonal ZrO_2 powders have the same physical characteristics as in Fig. 4c.

Irreversible transformation of tetragonal ZrO_2 to the monoclinic phase is also observed by grinding the powder mechanically. With continued grinding, the intensity of the reflections corresponding to $(1\,1\,1)_m$ and $(1\,1\,\bar{1})_m$ increases with simultaneous decrease in intensity of $(1\,1\,1)_t$. On grinding for ~3 h there was a 25% reduction in the tetragonal-phase content for the samples prepared in the presence of SO_4^{2-} ions. Under

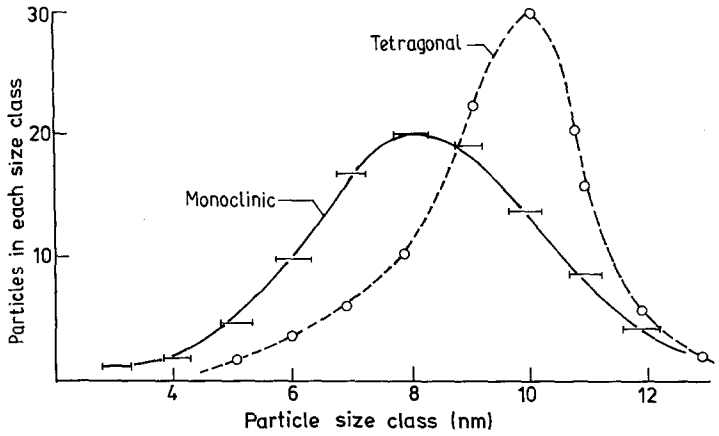

Figure 5 Size distribution curves derived from TEM studies for both tetragonal and monoclinic phases.

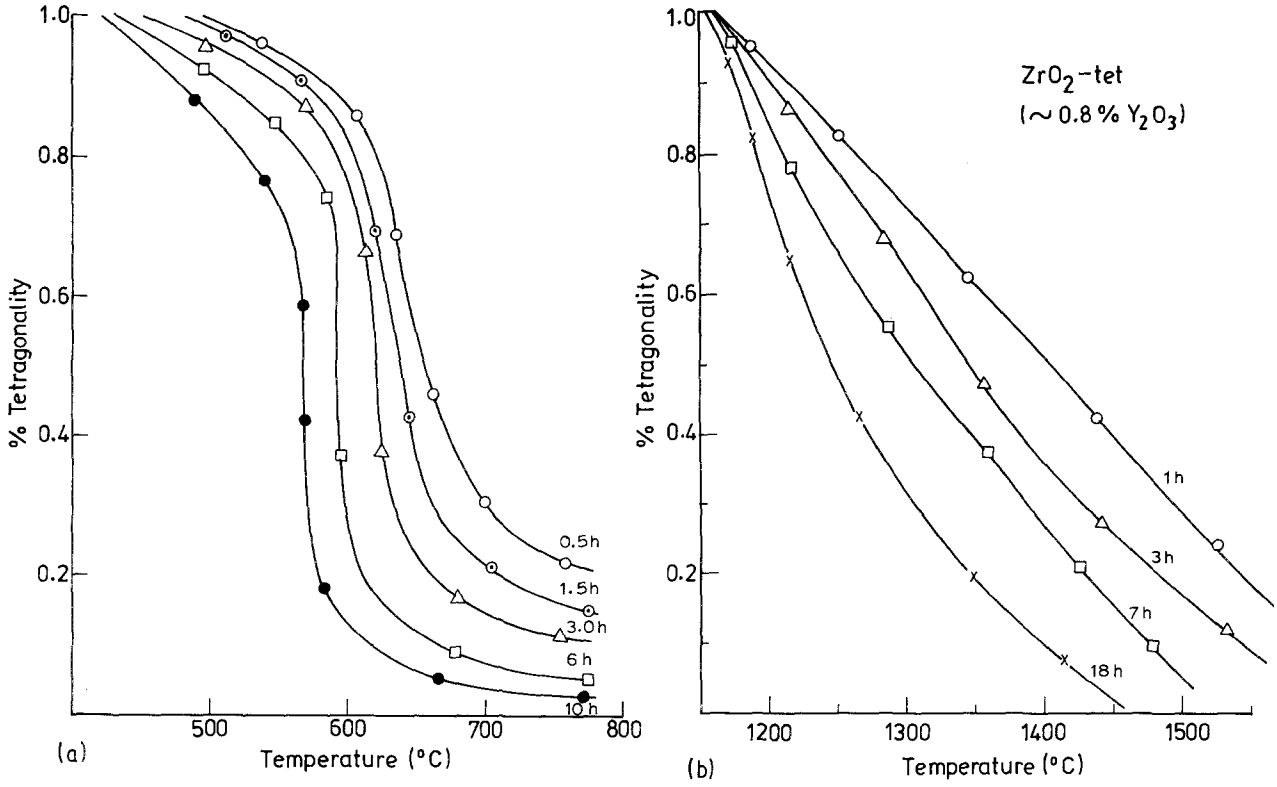

Figure 6 Kinetics of transformation behaviour of tetragonal to monoclinic phase for (a) ZrO_2 and (b) ZrO_2 + Y_2O_3.

the same conditions, the tetragonal ZrO_2 containing 0.8% Y_2O_3 showed a 10% to 15% reduction in tetragonality, provided the samples were initially annealed at 1150° C.

The transformation behaviour of tetragonal ZrO_2 containing 5% Y_2O_3 is found to be somewhat different. On thermal treatment above 1200° C it converts to the cubic phase (Fig. 7). Although the major peaks of tetragonal and cubic phases overlap, the absence of splitting in most of the lines such as (2 0 0), (2 2 0), (3 1 1) and (4 0 0) clearly indicate the transformation from tetragonal to cubic ZrO_2. The effects of mechanical grinding on samples with high Y_2O_3 contents are found to be very sluggish towards tetragonal–cubic transformations.

3.6. Fine powders of $MZrO_3$ (M = Ba, Sr or Ca)

$BaZrO_3$ is formed from the reaction between ultrafine ZrO_2 (monoclinic) and $Ba(OH)_2$ solution under hydrothermal conditions within 4 h at 185° C. This is in contrast to the hydrothermal formation of $BaZrO_3$,

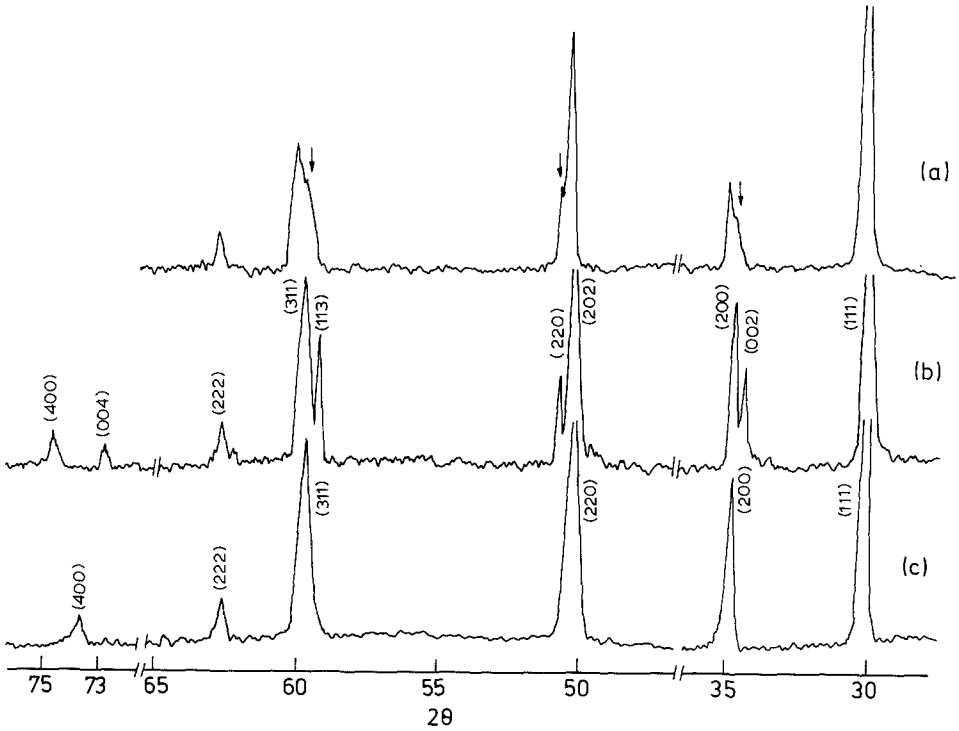

Figure 7 Part of the X-ray diffraction patterns showing the transition from tetragonal to cubic ZrO_2 as Y_2O_3 is added. (a) As-prepared ZrO_2 containing 4% Y_2O_3 showing tetragonal phase, (b) ZrO_2 with 0.8% Y_2O_3 heated to 1150° C and fast quenched, and (c) ZrO_2 with 6% Y_2O_3 heated to 1200° C showing predominantly cubic phase.

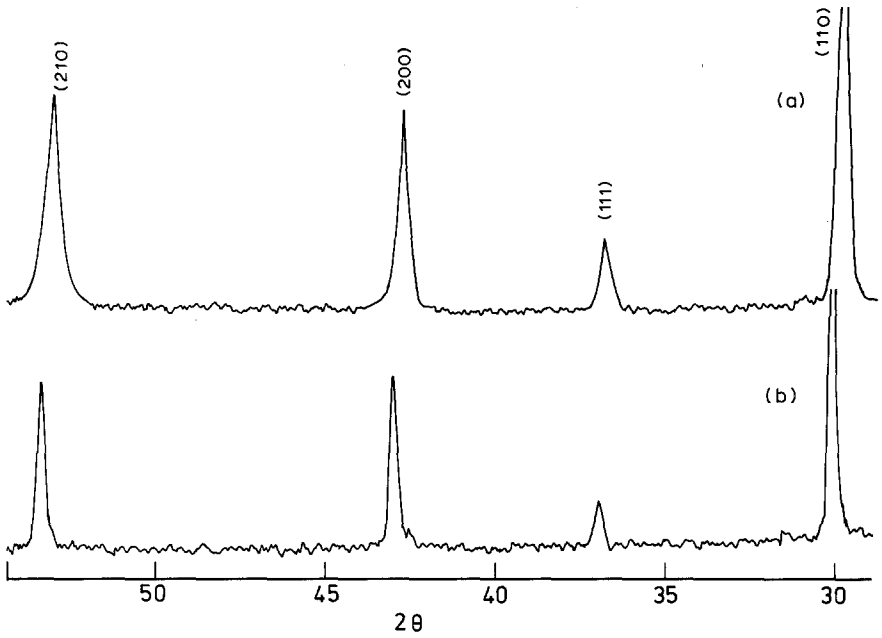

Figure 8 Part of the X-ray diffraction pattern of $BaZrO_3$ (a) as-prepared, and (b) after heating at 1000° C.

from $ZrO_2 \cdot nH_2O$ (n = 3 to 8) and $Ba(OH)_2$ at 130° C within 6 h [2]. The duration of the present reaction can be shortened to 2 h at 230° C. The X-ray powder diffraction pattern of this free-flowing powder corresponds to the cubic phase with a_0 = 0.419 nm (Fig. 8). The as-prepared samples show the least line broadening, indicating that the crystallite size is much larger than that of ZrO_2 particles. Combined DTA/TGA analysis in air shows the hydrothermal $BaZrO_3$ powder weight loss of 0.38% at 220 to 350° C with a broad endotherm. The weight remains unchanged up to 1200° C. After heat treatment at 1200° C for 2 h the cell constant of $BaZrO_3$ decreases to a_0 = 0.4188 nm. This is evident from the shift in all the X-ray reflections to somewhat higher 2θ values (Fig. 8). TEM studies reveal that $BaZrO_3$ particles have a nearly spherical shape (Fig. 10a). The diameter of the individual crystallites ranges from 0.08 to 3 μm. The electron diffraction patterns indicate the single-crystal nature of these particles with monodomain features (Fig. 10b). Nearly identical characteristics in X-ray diffraction, particle size and shape were observed for $BaZrO_3$ powder produced from ZrO_2 (tetragonal) and $Ba(OH)_2$ under hydrothermal conditions.

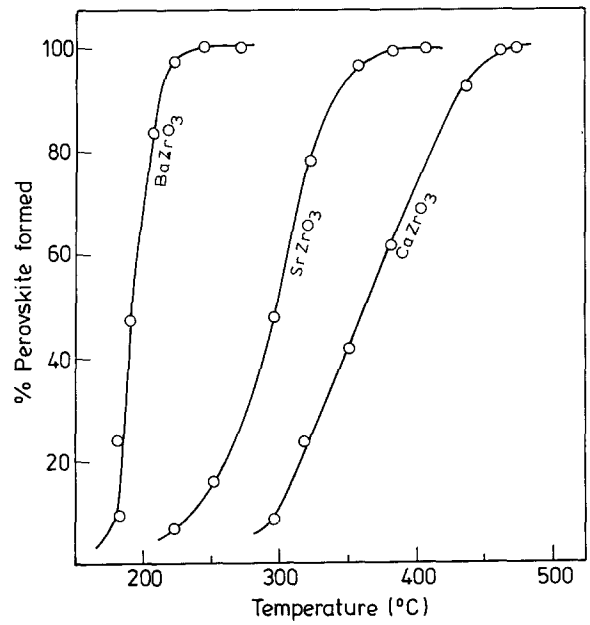

Figure 9 Kinetics of formation of $BaZrO_3$, $SrZrO_3$ and $CaZrO_3$ after a reaction time of 5 h.

Hydrothermal formation of $SrZrO_3$ from ZrO_2 (monoclinic) ultrafine powders and $Sr(OH)_2$ is incomplete even at 280° C after 10 h. Because this is the upper limiting temperature at which teflon-lining can be used, the reactions at 280 to 480° C were carried out directly in the stainless steel autoclave. The formation of $MZrO_3$ is kinetically controlled because increasing the temperature as well as time enhances the fraction of ZrO_2 converted to $MZrO_3$ (Fig. 9). Formation of $SrZrO_3$ is nearly complete at 360° C within 5 h. However, the reaction temperature must be enhanced to > 450° C for $CaZrO_3$ formation. The decreased reactivity may be related to the slow rate of conversion of CaO to $Ca(OH)_2$ in the hydrothermal fluids as compared to $Ba(OH)_2$. The X-ray powder diffraction pattern of $SrZrO_3$ and $CaZrO_3$ showed that both phases could be indexed on the basis of the orthorhombic unit cell with a_0 = 0.5814, b_0 = 0.8196 and c_0 = 0.5792 nm for $SrZrO_3$. The observed unit cell parameters for $CaZrO_3$ are a_0 = 1.1155, b_0 = 0.8003 and c_0 = 1.1494 nm. TEM observations reveal that $SrZrO_3$ particles are irregular shaped platelets of 0.1 to 0.5 μm size. The electron diffraction patterns show that these are monocrystalline. $CaZrO_3$ particles are mostly of rectangular prism shape with 0.2 to 1 μm length with an aspect ratio of 2 to 5. They are monodomain crystallites as indicated by the electron diffraction patterns.

4. Discussion

Crystallization of different polymorphs of ZrO_2 by varying the $[SO_4^{2-}]/[Cl^-]$ ratio can be explained in terms of the behaviour of hydrated Zr^{4+} ions in acid solutions of HCl compared to H_2SO_4. The observation that the anions influence only the precipitation stage

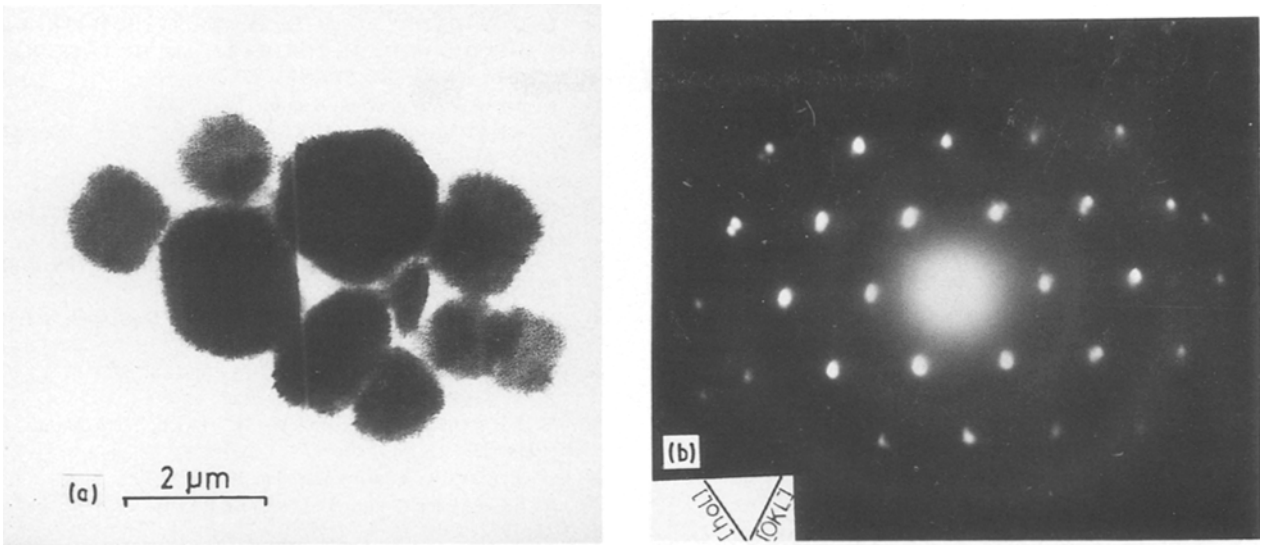

Figure 10 TEM of (a) $BaZrO_3$ and (b) selected-area electron diffraction of (a).

points to the relation between the nature of the molecular aggregation of Zr^{4+} ions and the stabilization of the specific ZrO_2 phase. Hydrolysed zirconium, often referred to as a zirconyl ion (ZrO^{2+}), is in fact the tetrametric species, $[Zr_4^{4+}(OH)_8(H_2O)_{16}]^{8+}$, present in the solid $ZrOCl_2 \cdot 8H_2O$ [30]. In strong HCl solution, Zr^{4+} ions exist as the trimer $[Zr_3(OH)_6Cl_3]^{3+}$ [31]. In both cases, Zr^{4+} ions are linked by pairs of hydroxo-bridges and are also bound to water molecules so that each zirconium is coordinated by eight oxygen atoms in a distorted square antiprismatic arrangement. In HCl solutions, part of the hydroxo-bridges are replaced by chlorine. These molecular species have a strong tendency to polymerize. The degree of polymerization increases with decreasing acid strength and is complicated by the slowness in attaining equilibrium as well as by the ageing of the solution [31]. Water in supercritical conditions, generally known as hydrothermal, exhibits different thermophysical, electrical and transport properties compared to water under ambient conditions [32]. Owing to changing solvation effects at elevated temperature and pressure, hydroxo-bridges in dissolved species convert to oxide-bridges so that ZrO_2 is formed during the last stage of polymerization. Elimination of the partially substituted chloro-bridges in these processes occurs towards the later stages, as evidenced by the presence of traces of chloride in the thermal analysis of ZrO_2 powder. This reaction sequence may influence the local symmetry giving rise to seven-coordinated zirconium ions as is the case in ZrO_2 (monoclinic).

Solutions of Zr^{4+} with sulphate as the anion show considerable differences in the molecular nature of aggregation, compared to those in a chloride-containing medium. Neutral complexes are present in this case, because crystals of $Zr(SO_4)_2 \cdot 4H_2O$ can be produced from 6 M H_2SO_4 solutions. This compound contains zirconium in a regular square antiprism surrounding each Zr^{4+} bound to four water and four sulphate groups which act as bridges to generate infinite sheets [33]. With the changed properties of solvent under hydrothermal conditions, bridged oxygens take the place of other anions to give rise to a higher symmetry environment of Zr^{4+}, as in tetragonal ZrO_2. Once the tetragonal phase is produced, it will not transfer to ZrO_2 (monoclinic) within the temperature range currently employed for the hydrothermal reaction. This is in contrast to the transformation reported in a strongly alkaline medium [16]. The high concentration of residual hydroxyls in tetragonal ZrO_2 also points to the difference in the polymerization process in the presence of SO_4^{2-} ions.

The residual hydroxyl ions have considerable influence on the metastability and phase equilibrium of oxides of tetravalent heavy elements as discussed by Mumpton and Roy [34]. Although free of cation impurities, tetragonal ZrO_2 can retain the hydroxyls at domain boundaries and in the surface region. The predominant multidomain nature of the hydrothermally prepared ZrO_2 (tetragonal) particle may be explained on this basis. Whereas single-domain tetragonal crystallites may transform more easily to the monoclinic phase, polydomain particles are more resistant to martensitic transformations. The difference in the shapes of the transformation kinetics can (Fig. 6) be accounted for in terms of cationic impurity substitution at the zirconium sublattice and thus differ from the domain boundary stabilization by hydroxyl ions.

Ultrafine powders of ZrO_2 can easily be surface hydroxylated which leads to the formation of colloidal suspensions at around neutral pH conditions. In basic solutions, the hydroxylation further penetrates into the bulk of the particles so that the Zr–O–Zr bridging bonds are disrupted, thereby collapsing the structure. This may lead to the formation of, at least partly, amorphous hydrated zirconia, $ZrO_2 \cdot xH_2O$. This may react with alkaline-earth metal ions giving rise to hydrated zirconates which crystallize to form anhydrous $MZrO_3$. However, a complete dissolution of amorphous $ZrO_2 \cdot xH_2O$ or $MZrO_3 \cdot yH_2O$ is not possible in weak alkaline solutions of $M(OH)_2$. The original morphology of ZrO_2 (monoclinic) crystallites is not retained by $MZrO_3$ particles, which rules out the possibility that the crystallite to crystallite (topotactic) conversion of ZrO_2 to $MZrO_3$ is taking place. On the

other hand, the M^{2+} ions entering the hydrated ZrO_3 phase produce chemical changes accompanied by dehydroxylation and heterogeneous nucleation of the zirconates. However, the effective rate of breaking the Zr–O–Zr bridging bonds depends on the basicity of $M(OH)_2$ which decreases with decreasing ionic size of M^{2+}. Therefore, the reaction of $Ca(OH)_2$ with ultrafine ZrO_2 requires much higher temperatures than the corresponding reaction with $Ba(OH)_2$. It is well known that ZrO_2 is more basic than TiO_2 and is therefore virtually insoluble in excess base. Thus the reaction paths in the hydrothermal formation of zirconate perovskite may not be identical to those in the case of $MTiO_3$ formation [7, 8].

References

1. T. R. N. KUTTY and R. BALACHANDRAN, *Mater. Res. Bull.* **19** (1984) 1479.
2. R. VIVEKANANDAN, S. PHILIP and T. R. N. KUTTY, *ibid.* **22** (1987) 99.
3. T. R. N. KUTTY and R. VIVEKANANDAN, *Mater. Lett.* **5** (1987) 79.
4. M. AVUDAITHAI and T. R. N. KUTTY, *Mater. Res. Bull.* **22** (1987) 641.
5. T. R. N. KUTTY and R. VIVEKANANDAN, *ibid.* **22** (1987) 1457.
6. R. VIVEKANANDAN and T. R. N. KUTTY, *Ceram. Int.* **14** (1988) 207.
7. *Idem, Powder Technol.* **57** (1989) 181.
8. T. R. N. KUTTY, R. VIVEKANANDAN and P. MURUGARAJ, *Mater. Chem. Phys.* **19** (1988) 533.
9. R. C. GARVIE, R. H. J. HANNINK and R. T. PASCOE, *Nature* **258** (1975) 703.
10. R. C. GARVIE and M. V. SWAIN, *J. Mater. Sci.* **20** (1985) 1193.
11. R. W. CYPRES and J. RAUCQ, *Ber. Deut. Keram Ges.* **40** (1963) 527.
12. A. CLEARFIELD, *Inorg. Chem.* **3** (1964) 146.
13. G. L. CLARK and D. H. REYNOLDS, *Ind. Eng. Chem.* **29** (1937) 711.
14. E. D. WHITNEY, *Trans. Faraday Soc.* **61** (1965) 1991.
15. T. MITSUHASHI, M. ICHIHARA and T. TATSUKE, *J. Amer. Ceram. Soc.* **57** (1974) 97.
16. N. NISHIZAWA *et al., ibid.* **65** (1982) 343.
17. A. KRAUTH and H. MEYER, *Ber. Deut. Keram. Ges.* **42** (1965) 61.
18. R. C. GARVIE, *J. Phys. Chem.* **69** (1965) 1238.
19. K. S. MAZDIYANSI, C. T. LYNCH and J. S. SMITH, *J. Amer. Ceram. Soc.* **48** (1965) 372.
20. J. E. BAILEY *et al., Trans. J. Brit. Ceram. Soc.* **71** (1972) 25.
21. H. RAU and T. R. N. KUTTY, *Ber. Bunsenges. Phys. Chem.* **76** (1972) 645.
22. H. TORAYA, M. YOSHIMURA and S. SŌMIYA, *J. Amer. Ceram. Soc.* **67** (1984) C-119.
23. G. K. WILLIAMSON and W. H. HALL, *Acta Metall.* **1** (1953) 22.
24. G. ZIEGLER, *Powder Met. Int.* **10** (1978) 70.
25. B. E. WARREN and B. L. AVERBACH, *J. Appl. Phys.* **23** (1952) 1959.
26. R. DELHEZ and E. J. MITTEMEIJER, *J. Appl. Crystallogr.* **9** (1979) 233.
27. A. R. STOKES, *Proc. Phys. Soc.* **B61** (1948) 382.
28. T. K. GUPTA *et al., J. Mater. Sci.* **12** (1977) 2421.
29. R. H. J. HANNINK *et al.*, in "Advances in Ceramics", Vol. 3, edited by A. H. Hener and L. W. Mobbs (American Ceramic Society, Ohio, 1981) p. 116.
30. A. CLEARFIELD and P. A. VAUGHAN, *Acta. Crystallogr.* **9** (1956) 555.
31. R. L. ANGSTADT and S. Y. TYREE, *J. Inorg. Nucl. Chem.* **24** (1962) 917.
32. E. U. FRANCK, in "Proceedings of the 1st International Symposium on Hydrothermal Reactions", edited by S. Sōmiya (Associates Sci. Doc. Inf., Tokyo, 1983) p. 1.
33. J. D. SINGER and D. J. CROER, *Acta. Crystallogr.* **12** (1959) 719.
34. A. MUMPTON and R. ROY, *J. Amer. Ceram. Soc.* **43** (1960) 234.

Received 6 April
and accepted 28 September 1989